

Extensive Comparison Results of Coverage Map of Optimum Base Station Location of Digital Terrain with UTD Based Model

Mehmet B. Tabakcioglu*

Abstract—In order to provide high quality of service broadcasting systems, predicting the electric field strength in all the receiving points and generating the coverage map of the transmitter are very important. Uniform Theory of Diffraction (UTD) based ray theoretical models could be used to predict the electric field and generate the coverage map in a short time. In order to eliminate the non-successive obstacles in the scenario and to reduce the computation time of UTD Model, Convex Hull (CH) technique is used for the first time. After this point, this model is named as Uniform Theory of Diffraction with Convex hull (UTD-CH) Model. Moreover, how operating frequency, obstacle height, and the distance between the obstacles affect the coverage map of optimum base station location are researched by using UTD based models. In this study, UTD, Slope Uniform Theory of Diffraction (S-UTD), Slope Uniform Theory of Diffraction with Convex Hull (S-UTD-CH), and UTD-CH models are used for comparisons. Furthermore, computation times of UTD based models are compared.

1. INTRODUCTION

Prediction of the electric field strength and generating the coverage map is vital for high quality of service (QoS) digital radio broadcasting systems. In order to supply this situation a great number of electromagnetic wave propagation models have been proposed along the history. Geometrical optics (GO) model was used to predict the electric field strength previously. GO model can explain the reflected and direct fields. However, GO model cannot calculate the field strength accurately behind an obstacle owing to that GO model does not explain the diffracted fields. In order to solve the diffracted field problem of GO model, Geometrical Theory of Diffraction (GTD) model is studied by [1–3]. Also it is asserted that diffracted wave is uniform in [4]. GTD model is an extension to GO model by adding extra diffracted waves. GTD model has failed to calculate the electric fields in the vicinity of the optical boundaries [5, 6]. Uniform Theory of Diffraction (UTD) model is proposed by Kouyoumjian and Pathak as an extension to GTD model in order to reduce the erroneous results at the optical boundaries [7]. UTD model loses the accuracy of predicted electric field strength as the observation, diffraction, and source points are close to the same line [8]. In other words, if the obstacle is in the transition zone of the previous ones, UTD model loses the accuracy [9]. Some UTD based simulation tools like FEKO and Winprop are also used to find coverage map and calculate the electric field [10, 11]. Another model is proposed to remove the penalty of UTD model for curved structures [12]. By this model, curved structure can be modeled more exactly. In order to remove the discontinuity and error of UTD model in the transition zone, Slope Uniform Theory of Diffraction (S-UTD) model is introduced with adding extra derivative terms [13–15]. As the diffraction number increases, S-UTD model loses the accuracy of predicting of the electric field strength [16]. In order to solve the computation time and accuracy problem of S-UTD model, Slope Uniform Theory of Diffraction with Convex Hull (S-UTD-CH) model is introduced for knife-edge and wedge type obstacle [17, 18]. If the obstacles heights in a given scenario

Received 4 August 2020, Accepted 11 September 2020, Scheduled 29 September 2020

* Corresponding author: Mehmet Baris Tabakcioglu (mehmet.tabakcioglu@btu.edu.tr).

The author is with the Electrical Electronics Engineering Department, Bursa Technical University, Bursa 16310, Turkey.

are close to each other, Slope UTD and Slope UTD with Convex hull models obtain approximately the same outcomes [19, 20].

In this paper, Uniform Theory of Diffraction with Convex Hull (UTD-CH) model is firstly presented, and extensive simulation results of comparison of models are provided. UTD-CH model is based on convex hull and Fresnel zone concept. Firstly, Fresnel zone is drawn between the transmitter and receiver, and then some nonsuccessive obstacles outside the zone are excluded from the scenario. After the exclusion of some obstacles, the previously mentioned convex hull is constructed with the rest obstacles as explained in [17]. Finally, UTD algorithm runs for the convex hull. Moreover, in this paper, UTD, S-UTD, S-UTD-CH, and UTD-CH models are compared regarding to operating frequency, distance between the obstacles, obstacle height, and computation time. This article is structured as follows. UTD based models like UTD Model, S-UTD Model, S-UTD-CH Model, and UTD-CH Model are briefly introduced in Section 2, and the simulation results are discussed and inter-compared in Section 3, followed by the Conclusions.

2. UTD BASED MODELS

In order to solve the electric field prediction problem, a lot of electromagnetic wave propagation models based on ray theoretical and numerical integration are proposed. UTD models are ray theoretical and based on ray tracing techniques. In this paper, classical UTD, S-UTD, S-UTD-CH, and UTD-CH models are briefly explained.

2.1. UTD Model

Electric field behind an obstacle is expressed in [9]

$$E = E_i D A(s) e^{-jks} \quad (1)$$

E_i is the incident electric field, D the diffraction coefficient, A the spreading factor, k the wave number, and s the travelling distance. The diffraction coefficient is given in [9]

$$D = -\frac{e^{-\frac{j\pi}{4}}}{2\sqrt{2\pi k} \cos\left(\frac{\alpha}{2}\right)} F\left[2kL \cos\frac{\alpha^2}{2}\right] \quad (2)$$

$F[\]$ is the transition function and given in [21]. L is the distance parameter for the diffraction coefficient. α is the diffraction angle as shown in Fig. 1. A is the spreading factor, and it is expressed as

$$A(s) = \sqrt{\frac{s_0}{s_1(s_1 + s_0)}} \quad (3)$$

s_0 and s_1 are the propagation distance of the wave before and after the diffraction, respectively.

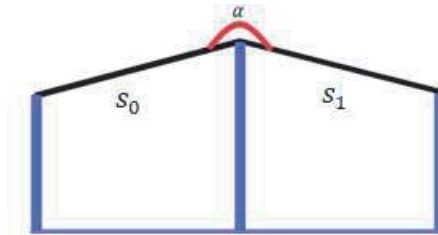


Figure 1. The diffraction scene.

2.2. S-UTD Model

Albeit UTD model is the fastest model in calculating electric field and coverage predicting, and it loses the accuracy in the transition region. Electric field behind an obstacle is expressed in [9]

$$E = \left[E_i D + \frac{\partial E_i}{\partial n} d_s \right] A(s) e^{-jks} \quad (4)$$

where d_s is the slope diffraction coefficient proposed in [9]

$$d_s = -\frac{e^{-j\frac{\pi}{4}}}{\sqrt{2\pi k}} L_S \sin(\alpha/2) \left(1 - F \left[2kL \cos \frac{\alpha^2}{2} \right] \right) \quad (5)$$

$F[\]$ is the transition function, k the wave number, L distance parameter for diffraction coefficient, L_s the distance parameter for the slope diffraction, and α the diffraction angle.

2.3. S-UTD-CH Model

Because obstacle number in the scenario increases, computation time and complexity increases with using S-UTD model. In order to decrease the computation time and complexity, S-UTD-CH, combination of two well-known models which are S-UTD and CH model, model is introduced [18]. Convex hull technique is applied to eliminate the non-successive obstacle in the scenario [22]. Convex hull technique is based on ellipsoid Fresnel zone concept. The radius of the Fresnel zone has an important role in eliminating the non-successive diffracting obstacles. In the case of one obstacle elimination, elapsed time is reduced to one fifth [23].

2.4. UTD-CH Model

This model is an improved version of the UTD model by using CH model. UTD-CH Model based on Fresnel zone between the transmitter and receiver as S-UTD-CH model. By using the Fresnel zones, non-successive diffracting obstacles are excluded from the scenario as illustrated in Fig. 2. UTD-CH model gives almost the same results with UTD model as seen in the simulation parts because non-successive obstacles are excluded from the scenario.

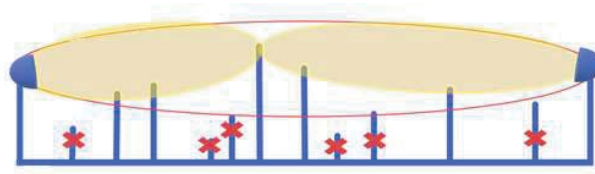


Figure 2. Construction of Convex hull.

3. SIMULATION RESULTS AND DISCUSSIONS

Coverage maps of optimum base station location by using UTD, S-UTD, S-UTD-CH, UTD-CH models with developed program in MATLAB (2016a) environment are inter-compared according to computation time and accuracy of prediction in certain digital terrain scenario. In the simulation, a laptop having 8 GB RAM and Intel i7-5500U processor is used. For the simulation, 121-building scenario is used as depicted in Fig. 3.

Obstacles heights in the terrain scenario are distributed randomly between 19 and 21 m as illustrated in Table 1.

In order to find the optimum base station location, at first, it is assumed that the base station location is (1, 1), and coverage map is generated for this place. Then (1, 2) position is selected as the base station location, and another coverage map is generated. This process continues until all the buildings are selected as the base station location. Finally, one of the coverage maps having the highest path loss value is selected as the coverage map of the optimum base station location. 20 and 50 m distance is provided between the obstacles. Moreover, frequencies are chosen 1800 MHz and 2100 MHz, respectively. How the frequency, distance between the buildings, building height distribution effects the coverage map and computation time is analyzed.

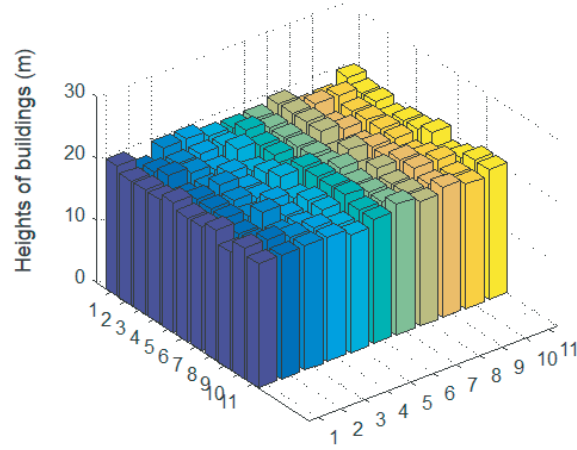


Figure 3. The digital terrain.

Table 1. Building heights.

21	19	21	21	20	20	20	21	19	19	21
20	20	20	20	20	21	20	21	21	21	20
20	21	20	19	21	20	20	21	19	20	20
20	19	19	20	19	20	20	21	20	20	19
21	20	21	19	20	19	20	19	19	20	20
20	20	20	19	21	21	20	21	20	20	20
20	20	19	20	19	21	21	19	20	19	21
21	19	21	19	20	21	20	21	21	20	19
19	19	19	19	20	21	20	20	21	21	20
21	21	20	20	19	20	20	20	20	20	21
20	20	20	20	19	20	21	20	21	20	21

3.1. Frequency Effect

In order to see the effects of frequency, the scenario in Fig. 3 is used. The distance between the buildings is 20 m. In comparison, UTD model is used. Operating frequency is selected as 1800 MHz and 2100 MHz, respectively. Firstly, 1800 MHz is selected, and the coverage map of optimum base station location is given in Fig. 4.

As can be seen in Fig. 4, optimum base station location is selected as $(x, y) = (6, 6) = (100 \text{ m}, 100 \text{ m})$. Path loss is decreased to -30 dB after 10 diffractions. As the second case, the frequency is selected as 2100 MHz, and the coverage map of optimum base station location is given in Fig. 5.

As seen in Fig. 5, optimum base station location is selected as $(x, y) = (5, 3) = (80 \text{ m}, 40 \text{ m})$.

3.2. Model Effect

Used model can affect the optimum base station location and coverage map. In order to verify this assertion, the distance between the obstacles and the frequency are selected as 50 m and 2100 MHz, respectively. Firstly, UTD model runs, and the coverage map of optimum base station is generated as demonstrated in Fig. 6.

As demonstrated in Fig. 6, optimum base station location is selected as $(x, y) = (5, 3) = (200 \text{ m}, 100 \text{ m})$. Path loss is reduced to -30 dB after several diffractions. Secondly, S-UTD model runs, and the

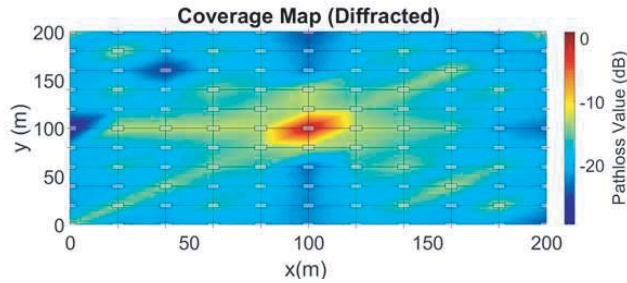


Figure 4. Coverage map of 1800 MHz, distance: 20 m.

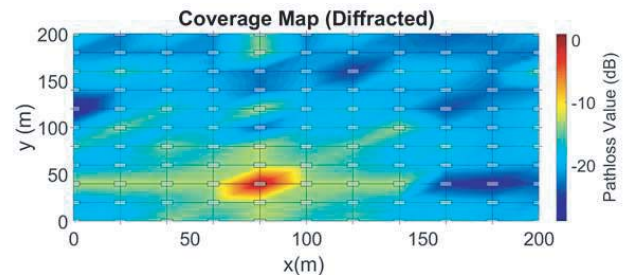


Figure 5. Coverage map of 2100 MHz, distance: 20 m.

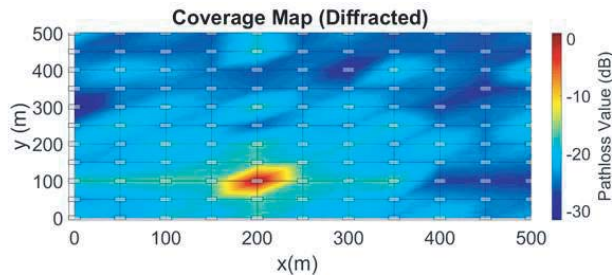


Figure 6. Coverage map of UTD Model.

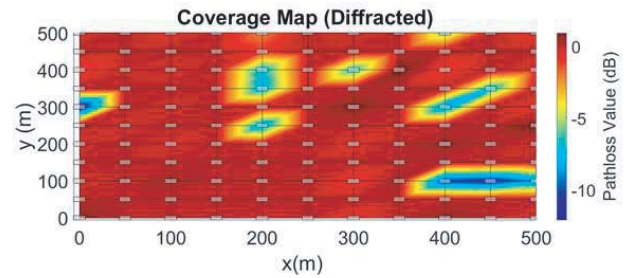


Figure 7. Coverage map of S-UTD Model.

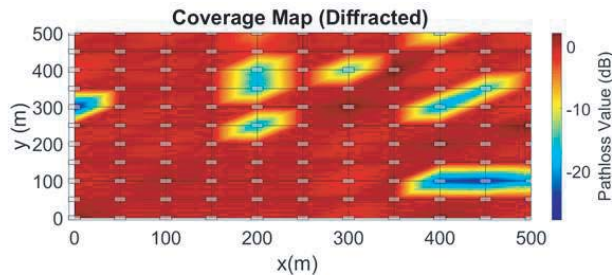


Figure 8. Coverage map of S-UTD-CH Model.

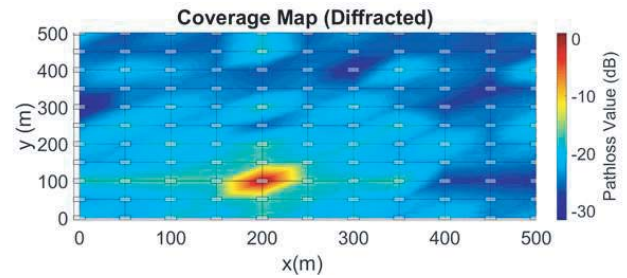


Figure 9. Coverage map of UTD-CH Model.

coverage map of optimum base station is generated as shown in Fig. 7.

As shown in Fig. 7, optimum base station location is selected as $(x, y) = (7, 5) = (300 \text{ m}, 200 \text{ m})$. Coverage map is changed completely as regard to Fig. 6 because slope terms are added in Slope UTD model. Path loss is reduced by -15 dB at most. As the heights of obstacles are close to each other, one obstacle is the transition zone of previous one. Therefore, UTD fails in that case. As seen in Fig. 6, most of the values are smaller than -20 dB . On the contrary, as can be seen in Fig. 7, most of the values are greater than -5 dB . Third, S-UTD-CH model runs, and the coverage map of optimum base station is indicated in Fig. 8.

As indicated in Fig. 8, optimum base station location is selected as $(x, y) = (7, 5) = (300 \text{ m}, 200 \text{ m})$. S-UTD and SUTD-CH models give almost the same coverage map because there is no building elimination, and all the buildings are in the transition region of previous buildings. Finally, UTD-CH model runs, and the coverage map of optimum base station is depicted in Fig. 9.

As depicted in Fig. 9, optimum base station location is selected as $(x, y) = (5, 3) = (200 \text{ m}, 100 \text{ m})$. UTD and UTD-CH models give almost the same coverage map because there is no non-successive building in the scenario. All the buildings are in the first Fresnel zone; therefore, it cannot be excluded from the scenario.

3.3. Building Space Effect

The distance between the buildings in the scenario also affects the coverage map of optimum base station location. In order to confirm this assertion, the frequency is chosen as 1800 MHz. S-UTD model is used for comparison. Firstly, the distance between the buildings is selected as 20 m, and coverage map is generated as illustrated in Fig. 10.

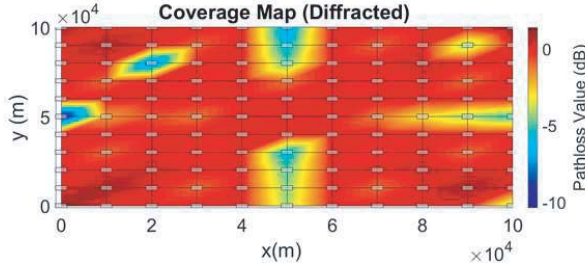


Figure 10. Distance: 20 m.

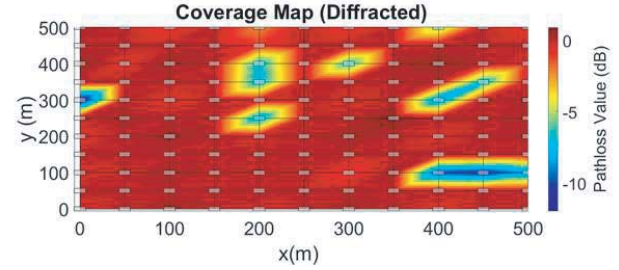


Figure 11. Distance: 50 m.

As illustrated in Fig. 10, optimum base station location is selected as $(x, y) = (6, 6) = (100 \text{ m}, 100 \text{ m})$. Moreover, path loss is reduced to -10 dB after several diffractions. At the second stage, the distance between the buildings is selected as 50 m, and the coverage map is demonstrated in Fig. 11.

As demonstrated in Fig. 11, optimum base station location is selected as $(x, y) = (7, 5) = (300 \text{ m}, 200 \text{ m})$. Due to the larger spacing between the buildings, path loss decreases to -15 dB .

3.4. Building Distribution Effect

In this case, obstacles heights in the terrain scenario are distributed randomly between 5 and 25 m as illustrated in Table 2.

Table 2. Building heights.

5	15	20	18	6	6	21	24	16	7	22
12	11	20	5	6	19	17	16	20	19	21
11	19	16	13	6	21	12	17	20	7	7
16	15	23	21	20	6	6	6	21	24	19
7	20	7	7	18	11	18	20	17	20	9
20	25	23	6	12	12	19	17	21	12	9
6	21	9	13	16	9	18	15	8	21	7
11	9	16	6	13	7	7	21	11	17	25
14	19	20	14	18	7	24	8	10	21	15
21	13	10	5	19	14	14	17	6	11	21
19	7	7	6	5	13	18	20	16	7	18

In order to highlight the effect of the building height distribution following scenario is considered. The frequency is chosen as 1800 MHz, and the distance between the obstacles is chosen as 20 m. As UTD model is run, coverage map of the optimum base station location is generated as seen in Fig. 12.

As seen in Fig. 12, optimum base station location is selected as $(x, y) = (4, 5) = (60 \text{ m}, 80 \text{ m})$. Moreover, most of the path loss value of the coverage is about -20 dB . Furthermore, it is reduced to -45 dB at most. For the same scenario, if S-UTD model is run, then the coverage map of the optimum base station location is generated as seen in Fig. 13.

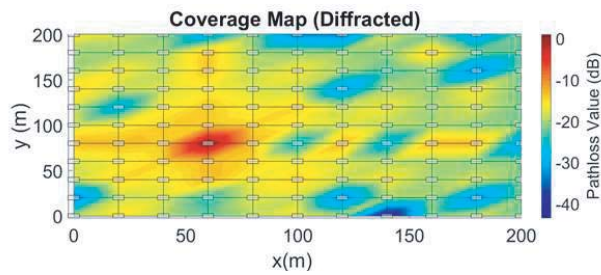


Figure 12. UTD Model.

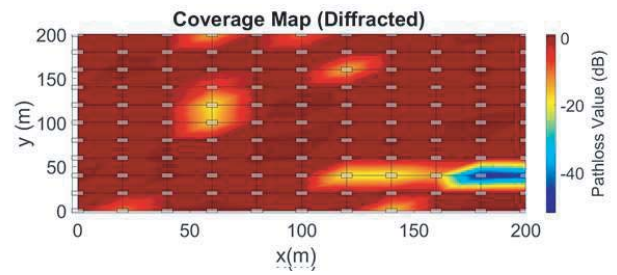


Figure 13. S-UTD Model.

As depicted in Fig. 13, the least path loss value in the coverage map is approximately the same as that in Fig. 12 because there is no slope term contribution in S-UTD model due to height variation in building heights.

3.5. Computation Time Comparison

In order to determine which model is the fastest, the scenario given in Table 2 is used. UTD based models like UTD, S-UTD, S-UTD-CH, and UTD-CH are used to make simulation, and elapsed times for the models are introduced in Table 3.

Table 3. Elapsed times of models.

UTD (s)	S-UTD (s)	S-UTD-CH (s)	UTD-CH (s)
15.6	334.1	327.5	21.1

As can be seen in Table 3, UTD model generates the coverage map of optimum base station location in the shortest time. Moreover, S-UTD model is the most unwieldy model thanks to contributing slope terms. Because the building height variation is low, there is no building elimination, and S-UTD-CH and S-UTD models give approximately the same elapsed time. Furthermore, in the same way, UTD and UTD-CH models generate the coverage map in close time.

4. CONCLUSIONS

Predicting the field strength and so generating the coverage map for optimum base station location is vital to seamless communication. UTD based ray theoretical models are faster than the numerical integration based models. Next, computation complexity of UTD based models is less than the numerical ones. Then, as the variation of building height distribution is large, UTD and UTD-CH models generate the coverage map in a short time. Adding slope diffraction terms S-UTD and S-UTD-CH models requires more time than other models with higher accuracy. Moreover, if the variation of the obstacle height is small, S-UTD and S-UTD-CH models obtain approximately the same results and elapsed times due to not eliminating any obstacles. In the same way, UTD and UTD-CH models obtain approximately the same results and elapsed times. Furthermore, convex hull technique is applicable in the high variety of height distribution.

ACKNOWLEDGMENT

This work is supported partially by TUBITAK (The Scientific and Technological Research Council of Turkey) under the grant No. 215E360.

REFERENCES

1. Keller, J. B., "Geometrical theory of diffraction," *J. Opt. Soc. Am.*, Vol. 52, 116–130, 1962.
2. Raman, C. V., "Caustics formed by diffraction and the geometric theory of diffraction patterns," *Proceedings of the Indian Academy of Sciences — Section A*, 307–317, 1959.
3. Kathavate, Y. V., "Geometric theory of Fresnel diffraction patterns," *Proceedings of the Indian Academy of Sciences — Section A*, Vol. 21, 77–87, 1945.
4. Kumar, R., "Structure of boundary diffraction wave revisited," *Appl. Phys. B*, Vol. 90, 379–382, 2008.
5. Luebbers, R. J., "Finite conductivity uniform gtd versus knife edge diffraction in prediction of propagation path loss," *IEEE Trans. Antennas and Propag.*, Vol. 32, No. 1, 70–76, 1984.
6. Schneider, M. and R. J. Luebbers, "A uniform double diffraction coefficient," *APS International Symposium*, Vol. 3, 1270–1273, 1989.
7. Kouyoumjian, R. G. and P. H. Pathak, "A uniform geometrical theory of diffraction for an edge in a perfectly conducting surface," *Proceedings of the IEEE*, Vol. 62, No. 11, 1448–1461, 1974.
8. Holm, P. D., "UTD-diffraction coefficients for higher order wedge diffracted fields," *IEEE Trans. Antennas and Propag.*, Vol. 44, No. 6, 879–888, 1996.
9. Tzaras, C. and S. R. Saunders, "An improved heuristic UTD solution for multiple-edge transition zone diffraction," *IEEE Trans. Antennas and Propag.*, Vol. 49, No. 12, 1678–1682, 2001.
10. Jakobus, U., A. G. Aguilar, G. Woelfle, J. Van Tander, M. Bingle, K. Longtin, and M. Vogel, "Recent advances of FEKO and WinProp," *APS URSI Science Meeting*, 409–410, 2018.
11. Shick, M., U. Jakobus, M. Schoeman, M. Bingle, J. Van Tandor, W. Burger, and D. Ludick, "Extended solution methods in FEKO to solve actual antenna simulation problems: Accelerated MoM and windscreen antenna modelling," *EUROP*, 3053–3055, 2011.
12. Kandimalla, D. and A. De, "High frequency uniform asymptotic solution for diffraction by the edges of a curved plate," *IEEE InCAP*, 1–4, 2018.
13. Andersen, J. B., "UTD multiple-edge transition zone diffraction," *IEEE Trans. Antennas and Propag.*, Vol. 45, No. 7, 1093–1097, 1997.
14. Andersen, J. B., "Transition zone diffraction by multiple edges," *IPMAP*, Vol. 141, No. 5, 382–384, 1994.
15. Rizk, K., R. Valenzuela, D. Chiznik, and F. Gardiol, "Application of the slope diffraction method for urban microwave propagation prediction," *IEEE VTC*, Vol. 2, 1150–1155, 1998.
16. Kara, A., H. L. Bertoni, and E. Yazgan, "Limit and application range of the slope-diffraction method for wireless communications," *IEEE Trans. Antennas and Propag.*, Vol. 51, No. 9, 2512–2514, 2003.
17. Tabakcioglu, M. B. and A. Kara, "Comparison of improved slope uniform theory of diffraction with some geometrical optic and physical optic methods for multiple building diffractions," *Electromagnetics*, Vol. 29, No. 4, 303–320, 2009.
18. Tabakcioglu, M. B. and A. Kara, "Improvements on slope diffraction for multiple wedges," *Electromagnetics*, Vol. 30, No. 3, 285–296, 2010.
19. Tabakcioglu, M. B., "S-UTD-CH model in multiple diffractions," *International Journal of Electronics*, Vol. 103, No. 5, 765–774, 2016.
20. Tabakcioglu, M. B., "A top-down approach to S-UTD-CH model," *ACES Journal*, Vol. 32, No. 7, 586–592, 2017.
21. Mcnamara, D. A., C. Pistorius, and J. Malherbe, *Introduction to the Uniform Geometrical Theory of Diffraction*, Artec House, Boston, 1990.
22. Chung, H. K. and H. L. Bertoni, "Application of isolated diffraction edge (IDE) method for urban microwave path loss prediction," *IEEE VTC*, Vol. 1, 205–209, 2003.
23. Tabakcioglu, M. B. and A. Cansiz, "Application of S-UTD-CH model into multiple diffraction scenarios," *International Journal of Antennas and Propagation*, 1–5, 2013.